nature neuroscience

Object-based attention involves the sequential activation of feature-specific cortical modules

Mircea A Schoenfeld[1–3], Jens-Max Hopf[1,2], Christian Merkel[1,2], Hans-Jochen Heinze[1,2] & Steven A Hillyard[2,4]

Object-based theories of attention propose that the selection of an object's feature leads to the rapid selection of all other constituent features, even those that are task irrelevant. We used magnetoencephalographic recordings to examine the timing and sequencing of neural activity patterns in feature-specific cortical areas as human subjects performed an object-based attention task. Subjects attended to one of two superimposed moving dot arrays that were perceived as transparent surfaces on the basis either of color or speed of motion. When surface motion was attended, the magnetoencephalographic waveforms showed enhanced activity in the motion-specific cortical area starting at ~150 ms after motion onset, followed after ~60 ms by enhanced activity in the color-specific area. When surface color was attended, this temporal sequence was reversed. This rapid sequential activation of the relevant and irrelevant feature modules provides a neural basis for the binding of an object's features into a unitary perceptual experience.

Our visual surroundings typically include a multitude of objects that differ in their locations, shapes and constituent features. Specific objects may be selected for detailed examination and perceptual enhancement by directing attention to their locations[1] or to their identifying features[2]. There is increasing evidence that attention may also select entire objects, including all of their constituent features, as integrated perceptual units[3,4]. Although a substantial amount of research has been conducted to examine the neural mechanisms of space-based and feature-based attention, only a few studies have investigated the neural mechanisms of object-based attention (for reviews, see refs. 3,5,6).

A major unsolved question regarding the neural mechanisms of object-based attention is how the different features of an attended object, which may be represented in widely dispersed cortical areas, are bound together to form a unified percept. A promising approach to this vexatious binding problem comes from the integrated competition model[7–9]. According to this model, directing attention to one of an object's features enhances neural activity in the cortical module encoding that feature, which then spreads to different modules that encode the other features of the object. The resulting activation of the entire network of specialized modules underlies the binding of the features of the attended object into a unified perceptual experience. This schema was extended in the incremental grouping model[10], which proposes that feature binding involves the time-consuming spread of enhanced neural activity across the network of visual areas that encode the features of an object or perceptual group via recurrent inter-areal connections.

A key prediction of object-based theories of attention is that directing attention to a particular feature of an object, such as its shape or color, results in the whole object being selected, including both its task-relevant and irrelevant features. Critical support for this proposition came from a functional magnetic resonance imaging study[11] that demonstrated that neural activity was increased not only in the cortical area that encoded an attended feature (for example, face or house shape), but also in the area encoding a task-irrelevant feature (for example, motion) of the attended object. Evidence from event-related potentials (ERP) and magnetoencephalographic (MEG) recordings[12] revealed that selection of a task-irrelevant feature could occur rapidly enough to be involved in the perceptual integration and binding of the multiple features of an attended object. What has yet to be demonstrated, however, is whether there is a rapid and sequential selection of the relevant followed by the irrelevant feature in their respective sensory modules, as postulated by both the integrated competition and incremental grouping models.

To examine this question, we analyzed the respective time courses of relevant and irrelevant feature selections by recording event-related magnetic fields (ERFs) in an object-based attention task. Subjects were cued to attend to one of two superimposed transparent moving surfaces either on the basis of its motion velocity (fast versus slow) or its color (red versus gray) (**Fig. 1**). Previous studies have shown that superimposed moving dot surfaces of this type have properties equivalent to those of multi-feature objects and may be attended as unitary feature ensembles[13–15]. Neural activity sources in the lateral occipital motion-sensitive area and the ventral occipital color-sensitive area were isolated, and their respective time courses were delineated under conditions in which each feature was relevant and in which it was irrelevant. We found that relevant and irrelevant features were selected in rapid sequence in their respective specialized cortical areas, thereby identifying a fundamental mechanism of object-selective attention.

RESULTS

Experiment 1: attend to surface defined by motion speed

Reaction times were faster (718 versus 762 ms) and hit rates were slightly higher (76.2 versus 74.8%) for targets belonging to the

[1]Department of Neurology, Otto-von-Guericke University, Magdeburg, Germany. [2]Department of Behavioral Neurology, Leibniz Institute for Neurobiology, Magdeburg, Germany. [3]Kliniken Schmieder, Allensbach, Germany. [4]Department of Neurosciences, University of California at San Diego, LaJolla, California, USA. Correspondence should be addressed to M.A.S. (ariel.schoenfeld@med.ovgu.de).

Received 21 October 2013; accepted 22 January 2014; published online 23 February 2014; doi:10.1038/nn.3656

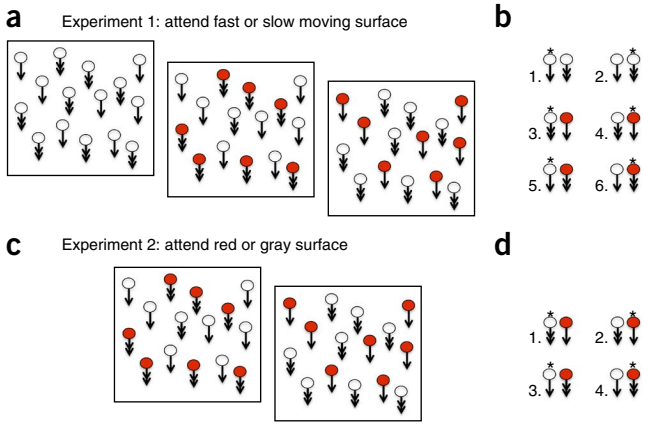

Figure 1 Stimuli for experiments 1 and 2. For experiment 1, the task was to attend to the fast- or slow-moving transparent surface. Color was irrelevant. (**a**) Schematic diagram of three possible stimulus configurations, which were presented equiprobably in random order. The fast or slow downwards moving dot arrays formed transparent surfaces that could be either red or gray. Single arrows indicate the slow-moving array and double arrows indicate the fast-moving array. A cue that appeared every 16–20 trials instructed the subject to attend to either the fast- or the slow-moving surface. Subjects responded with a button press to a short lateral displacement of the attended moving surface that occurred on some trials. (**b**) The six experimental conditions defined by the speed and color of the attended surfaces. * indicates the attended surface. For experiment 2, the task was to attend to the red or the gray moving transparent surface. Motion speed was irrelevant. (**c**) Schematic diagram of the two possible stimulus configurations. One of the transparent surfaces was always red and moved either fast or slow. Subjects were cued to attend either to the red or to the gray surface and to press a button on the occurrence of a lateral displacement of the attended moving surface. (**d**) The four experimental conditions defined by the color and speed of the attended surface.

fast-moving surface. The false alarm rates were 2.2% (for responses to lateral displacement of the slow surface while attending the fast surface) and 2.6% (for responses to lateral displacement of the fast surface while attending the slow surface). A repeated-measures ANOVA with two factors (surface speed and presence of a color change) revealed a significant main effect of surface speed for the reaction times ($F_{1,17} = 6.34$, $P = 0.02$) in the absence of a main effect for color-change presence ($F_{1,17} = 0.10$, $P = 0.75$). There was no significant interaction between these factors ($F_{1,17} = 0.12$, $P = 0.73$). A similar pattern was observed for the hit rates. Here, the repeated-measures ANOVA revealed a significant main effect for surface speed ($F_{1,17} = 6.41$, $P = 0.02$) in the absence of a main effect for color change ($F_{1,17} = 1.13$, $P = 0.30$). Again, there was no significant interaction between the factors ($F_{1,17} = 0.85$, $P = 0.36$). For false alarm rates, there was no significant main effect for surface speed ($F_{1,17} = 0.27$, $P = 0.61$) or color presence ($F_{1,17} = 0.87$, $P = 0.36$), and there was no interaction between these factors ($F_{1,17} = 1.36$, $P = 0.25$).

The sensory color effect was revealed by subtracting the gray-slow/gray-fast* (asterisk indicates the attended surface) ERF from the red-slow/gray-fast* ERF. This effect (**Fig. 2a**) started at 120 ms and was highly significant in the time range 120–250 ms at occipito-temporal sensors over the left ($F_{1,17} = 58.38$, $P = 0.00000068$) and right ($F_{1,17} = 46.84$, $P = 0.0000028$) hemispheres. Its sources were localized to the left and right inferior occipital cortex. The timing and the sources of this sensory color effect replicated earlier findings[9,15]. Talairach coordinates of these and other source localizations are given in **Table 1**.

We assessed the sensory motion effect by analyzing the N180m component elicited by the gray-slow*/gray-fast stimulus (**Fig. 2b**). This effect started at 120 ms and was highly significant over the time range 120–250 ms ($F_{1,17} = 38.56$, $P = 0.0000095$). Its sources were localized to the left and right middle occipital gyri, consistent with earlier findings that movement-evoked activity originates in the motion sensitive area V5/hMT[15,16].

The attentional selection of the fast- versus slow-moving surface was evident in the gray-slow/gray-fast* minus gray-slow*/gray-fast difference waveform as an enhanced ERF over lateral occipital sensors that started at 150 ms and remained significant until 350 ms ($F_{1,17} = 7.68$, $P = 0.013$; **Fig. 3**). The sources of this enhanced ERF signal were localized almost symmetrically in the left and right middle occipital gyri and were very similar to the sources of the sensory motion effect shown in **Figure 2b**.

The selection of the relevant motion-speed feature was also evident in the gray-slow/red-fast* minus gray-slow*/red-fast difference wave as an enhanced ERF over lateral occipital sensors (**Fig. 4a**). This effect was significant over 150–200 ms ($F_{1,17} = 8.86$, $P = 0.0085$), and its sources were localized to the middle occipital gyrus, in the same region as the sensory effect of motion (**Figs. 2b** and **3**, and **Table 1**). The timing, topographical distribution and source localization of this motion-based attention effect closely replicate previous findings in which attention to the feature of motion was studied using similar stimuli[17]. This motion-based attention effect was followed by an enhanced ERF signal over 220–350 ms ($F_{1,17} = 7.36$, $P = 0.015$) having

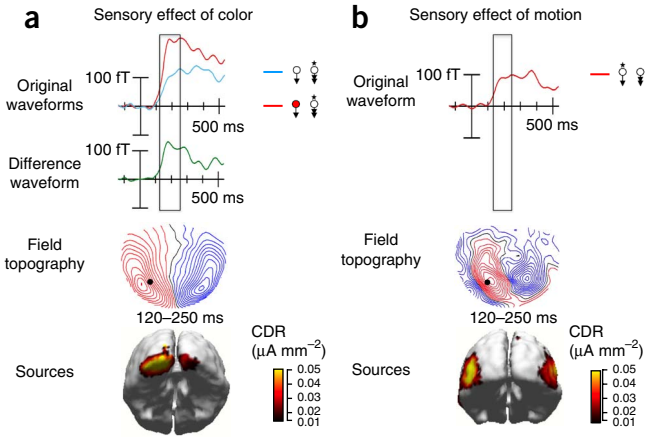

Figure 2 The sensory effects of color and motion. (**a**) The sensory effect of color ($N = 18$). ERF waveforms were averaged over all subjects on trials with no color change accompanying dot movement (blue tracing) and on trials in which the dots in the unattended slowly moving surface changed to red (red tracing). Time zero of recording epoch is when the dot arrays began to move. The difference waveform (green trace) was formed by subtracting the color-absent from the color-present waveform (shown above). Outline rectangle shows the time range in which the effect was significant at occipito-temporal sensors over the left ($F_{1,17} = 58.38$, $P = 0.00000068$) and right ($F_{1,17} = 46.84$, $P = 0.000028$) hemispheres. The topographical distribution of the difference ERF is shown below together with its estimated sources. (**b**) The sensory effect of motion ($N = 18$). ERF waveform (red trace) elicited by the color-absent stimulus while the slowly moving surface was attended (gray-slow*/gray-fast). The corresponding topographical distribution of the ERF in the time range 120–250 ms in which the effect was significant ($F_{1,17} = 38.56$, $P = 0.0000095$) and its estimated sources are shown below.

Table 1 Talairach coordinates of the modeled sources of neural activity in the different conditions of the two experiments

	Motion-sensitive areas			Color-sensitive areas		
	x	*y*	*z*	*x*	*y*	*z*
Experiment 1: sensory effect of color				−18	−83	−8
				9	−88	−8
Experiment 1: sensory effect of motion	−42	−75	5			
	50	−73	7			
Experiment: attend fast versus attend slow motion	−40	−78	4			
	52	−72	6			
Experiment 1: object-based attention effects						
Gray-slow*/red-fast minus gray-slow/red-fast*	−42	−82	6	−16	−81	−8
	57	−67	7	10	−85	−10
Gray-fast/red-slow* minus gray-fast*/red-slow	−44	−80	6	−17	−82	−8
	55	−66	6	8	−88	−8
Experiment 2: object-based attention effects						
Red-fast/gray-slow* minus red-fast*/gray-slow	−42	−79	8	−16	−92	−4
	54	−70	8	13	−84	−6
Red-slow/gray-fast* minus red-slow*/gray-fast	−45	−72	7	−20	−85	−5
	55	−74	8	10	−84	−6

a very different topography and bilateral sources in the ventral occipital cortex that closely resembled the sources of the sensory color effect (**Fig. 2a** and **Table 1**). Thus, this subsequent ERF deflection appears to reflect the selection of the irrelevant color feature, as the difference wave included an attend-red minus attend-gray comparison.

Similar sequential effects of relevant motion and irrelevant color selection were evident in the gray-fast*/red-slow minus gray-fast/red-slow* difference wave (**Fig. 4b**). In this case, the initial attention effect was also an enhanced ERF over the 150–200-ms interval ($F_{1,17} = 5.62$, $P = 0.03$) that was localized to the same lateral occipital area as the sensory effect of motion (**Fig. 2b** and **Table 1**). The subsequent ERF deflection over 220–350 ms ($F_{1,17} = 5.52$, $P = 0.03$) had a topographical distribution and source localization similar to that of the sensory color effect (**Fig. 2a** and **Table 1**). This deflection was a signal reduction, as expected, because the difference wave subtracts an attend-red condition from an attend-gray condition. Thus, for both sets of difference waves in the attend motion conditions shown in **Figure 4**, there was an initial motion-selective effect in the lateral occipital area followed after 50–70 ms by a color-selective modulation in the inferior occipital area.

Experiment 2: attend to surface defined by color

The reaction times did not differ significantly when subjects attended to the red versus the gray surface ($F_{1,11} = 1.164$, $P = 0.30$). However, reaction times were slightly faster (642 versus 668 ms) when the attended surface was moving fast versus slow ($F_{1,11} = 55.66$, $P = 0.000013$). A similar pattern was also observed for the hit rates (79% versus 76%, $F_{1,11} = 29.52$, $P = 0.0002$). There was no main effect of attending to red (77.6%) versus gray (77.8%) surfaces on hit rates ($F_{1,11} = 0.59$, $P = 0.46$). The false alarm rates did not differ ($F_{1,11} = 1.36$, $P = 0.27$) when subjects attended to the red (3.2%) versus the gray (3.4%) surface.

The initial selection of the relevant color feature was evident in the gray-slow/red-fast* minus gray-slow*/red-fast difference wave as an enhanced ERF in the time range 150–200 ms ($F_{1,11} = 12.88$, $P = 0.0043$; **Fig. 5a**) that was localized to the same inferior occipital areas as the sensory color effect (**Fig. 2a**, **Table 1**). The subsequent ERF deflection in the time range 220 – 350 ms ($F_{1,11} = 26.62$, $P = 0.00031$) had a different topographical distribution (**Fig. 5a**) and was localized to the same lateral occipital areas as the sensory motion effect (**Fig. 2b** and **Table 1**).

Similar sequential effects of relevant color and irrelevant motion selection were seen in the gray-fast/red-slow* minus gray-fast*/red-slow difference waves. The initial attention effect was an enhanced ERF over the 150–200-ms interval ($F_{1,11} = 14.84$, $P = 0.0027$) that was localized to the same inferior occipital region (**Fig. 5b**) as the sensory color effect (**Fig. 2a** and **Table 1**) and the attention to color effect (**Fig. 5a**). The subsequent ERF deflection over the 220–350-ms interval ($F_{1,11} = 18.92$, $P = 0.0012$) was a signal reduction that was expected because the difference wave subtracts an attend-fast condition from an attend-slow condition. The sources of the reduction were localized to the same bilateral occipital areas as the sensory effect of motion (**Fig. 2b** and **Table 1**).

Given that the foregoing analyses revealed bilateral sources located in the lateral middle occipital gyri associated with motion processing and in the occipital inferior cortex associated with color processing across the two experiments, we conducted an additional analysis in source space to delineate the precise timing of the activity in these regions in the different experimental conditions. For each difference waveform, the source waveforms of the left and right hemisphere homologous sources were averaged together over an epoch of 440 ms, resulting in one time course for each bilateral pair of sources (Online Methods). In experiment 1, the time course of the sensory effect of color was evident in the source difference waveform red-slow/gray-fast*

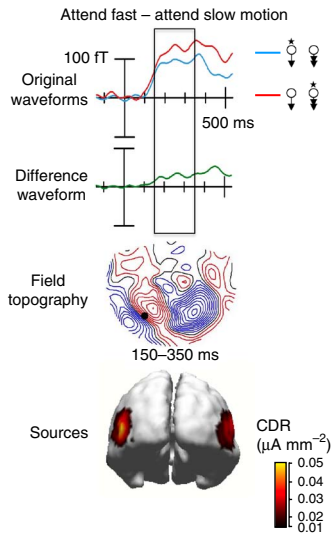

Figure 3 Effect of attention on motion processing in color-absent conditions. ERF waveforms on trials where subjects attended the fast moving surface (gray-slow/gray-fast*) are shown in red; those when subjects attended the slow surface (gray-slow*/gray-fast) are shown in blue ($N = 18$). The difference waveform (green) was formed by subtracting the attend-slow from attend-fast surface waveform. Outline rectangle indicates the time range (150–250 ms) in which the effect was significant ($F_{1,17} = 7.68$, $P = 0.013$). Bottom, the topographic distribution of the difference ERF during this time range is shown together with the estimated sources. Note the similarity between the topography and the source locations of this difference and those of the sensory motion effect in **Figure 2b**.

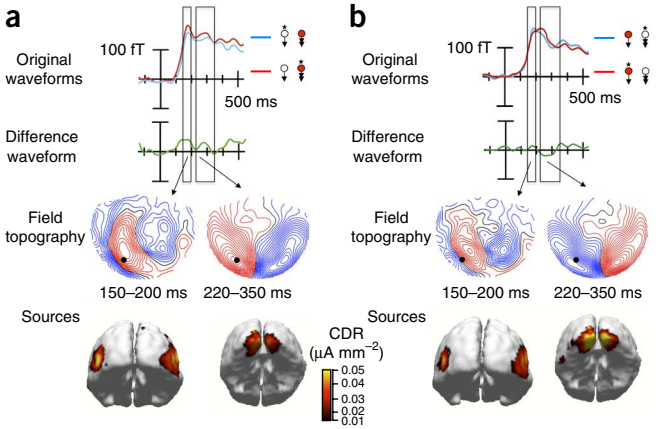

Figure 4 Experiment 1: sequential selection of attended motion feature and unattended color feature. (**a**) ERF waveforms elicited by the gray-slow/red-fast stimulus when the fast (red trace) versus the slow (blue trace) surface was attended ($N = 18$). The difference waveform (green trace) shown below was formed by subtracting the ERF on gray-slow*/red-fast trials from the ERF on gray-slow/red-fast* trials. Outline rectangles indicate the time ranges in which significant differences were observed. Topography and sources of early difference waveform (150–200 ms, $F_{1,17} = 8.86$, $P = 0.0085$) were very similar to those of motion sensory effect (**Fig. 2b**), whereas later differences (220–350 ms, $F_{1,17} = 7.36$, $P = 0.015$) were similar to color sensory effect (**Fig. 2a**). (**b**) ERF waveforms elicited by the gray-fast/red-slow stimulus when the slow (red trace) versus the fast (blue trace) surface was attended. The difference waveform (green trace) shown below was formed by subtracting the gray-fast/red-slow* trials from ERFs on the gray-fast*/red-slow trials. The outline rectangles indicate the time ranges in which significant differences were observed. As in **a**, the difference waveform shows sequential selections based on the relevant motion feature (at 150–200 ms, $F_{1,17} = 5.62$, $P = 0.03$) and then the irrelevant color feature (at 220–350 ms, $F_{1,17} = 5.52$, $P = 0.031$). Talairach coordinates for the color and motion sources are shown in **Table 1**.

minus gray-slow/gray-fast* (**Fig. 6a**). The sensory effect of motion was visualized in the source waveform of the ERF elicited by the gray-slow*/gray-fast stimulus (**Fig. 6a**). To visualize the object-based attention effects in experiment 1, we averaged together the source waveforms derived from the difference waves gray-slow/red-fast* minus gray-slow*/red-fast and gray-fast*/red-slow minus gray-fast/red-slow*; specifically, we averaged the two time courses from the motion sensitive areas and the two from the color sensitive areas, which resulted in one averaged time course for the motion sensitive areas and one for the color sensitive regions (**Fig. 6b**). Given that these source difference waveforms are based on current density measures, their values are all positive and therefore additive regardless of the signs of the difference wave comparisons (Online Methods).

To visualize the object-based attention effects in experiment 2, we averaged together the source waveforms derived from the gray-slow/red-fast* minus gray-slow*/red-fast and gray-fast/red-slow* minus gray-fast*/red-slow difference comparisons. As for the object-based attention effects in experiment 1, the two time courses from the motion sensitive areas and the two from the color sensitive areas were separately averaged (**Fig. 6c** and **Supplementary Figs. 1** and **2**).

The source activity for the sensory effect of color in the inferior occipital cortex began at 115 ms post-stimulus and for the sensory effect of motion in the middle occipital gyri at 125 ms (**Fig. 6a**). In experiment 1, where the surface was selected on the basis of motion speed, the source activity in the middle occipital motion area started to increase at 155 ms, whereas the source activity in the inferior occipital cortex started to increase 60 ms later (at 215 ms), reflecting selection of the irrelevant color feature (**Fig. 6b**). In experiment 2, where the surface was selected on the basis of color, source activity started first in the color-selective inferior occipital region starting at 160 ms, followed 65 ms later by activity in the motion-sensitive middle occipital gyri, reflecting selection of the irrelevant motion feature (**Fig. 6c**). The differences in latency between the relevant and irrelevant source waveform modulations shown in **Figure 6** were highly significant (experiment 1, $F_{1,17} = 76.42$, $P = 0.000000011$; experiment 2, $F_{1,11} = 58.66$, $P = 0.0000099$).

DISCUSSION

We used MEG recordings to track feature selection and integration processes in the brain during object-selective attention. Subjects attended to one of two superimposed moving dot arrays either on the basis of its color or its speed of motion. Such arrays are perceived as moving transparent surfaces and can be selectively attended as multi-feature objects[12–16]. The initial registration of sensory information in feature-specific cortical areas became significant at 115–120 ms after stimulus onset for color (in the ventral occipital color area) and at 125–130 ms for motion (in the lateral occipital motion area). Selection of the task-relevant feature (color or motion) was associated with a precisely timed modulation of neural activity beginning 30–40 ms after the initial sensory registration in the same specialized cortical

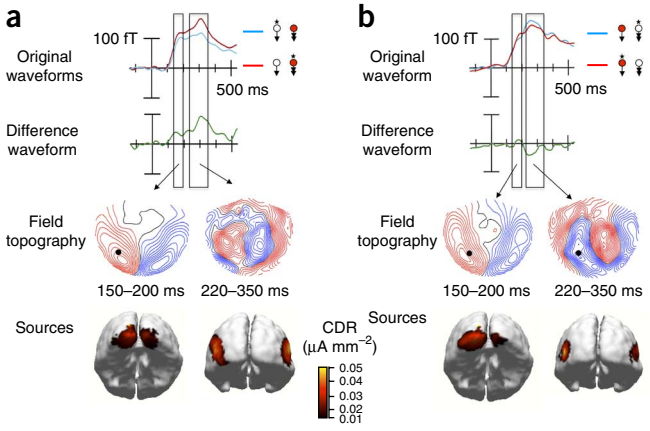

Figure 5 Experiment 2: sequential selection of attended color feature and unattended motion feature. (**a**) ERF waveforms elicited by the gray-slow/red-fast stimulus when the red (red trace) versus the gray (blue trace) surface was attended ($N = 12$). The difference waveform (green trace) was formed by subtracting the gray-slow*/red-fast trials from ERFs on gray-slow/red-fast* trials. The outline rectangles indicate the time ranges over which significant differences were observed. The topography and sources of the early difference (150–200 ms, $F_{1,11} = 12.88$, $P = 0.0043$) were very similar to those of the sensory color effect (**Fig. 2a**), and the later difference (220–350 ms, $F_{1,11} = 26.62$, $P = 0.00031$) to those of the sensory motion effect (**Fig. 2b**). (**b**) ERF waveforms elicited by the gray-fast/red-slow stimulus when the red (red trace) versus the gray surface (blue trace) was attended. The difference waveform (green trace) was formed by subtracting the gray-fast*/red-slow trials from ERFs on gray-fast/red-slow* trials. As in **a**, the difference waveform shows sequential selections based on the attended color feature (150–200 ms, $F_{1,11} = 14.84$, $P = 0.0027$) and the irrelevant motion feature (220–350 ms, $F_{1,11} = 18.92$, $P = 0.0012$). Talairach coordinates of the source localizations are given in **Table 1**.

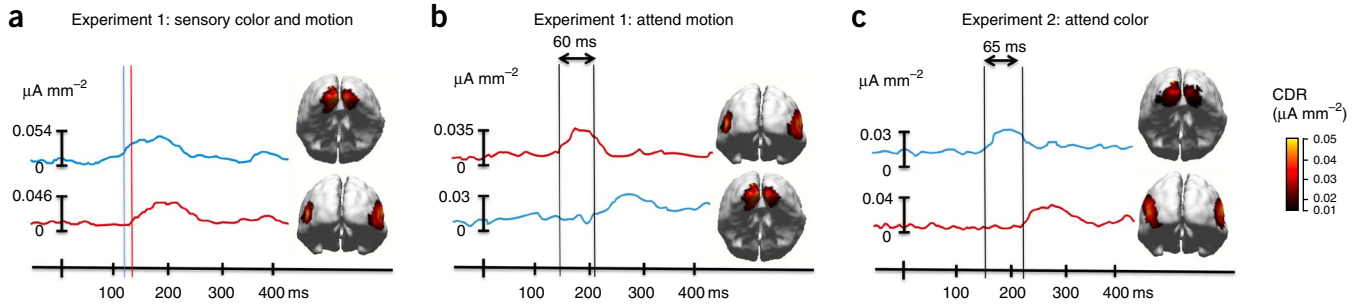

Figure 6 Source waveforms showing timing of sensory effects and relevant and irrelevant feature selections. Note that all waveform deflections are positive (upwards) regardless of the sign of the subtractions, as these waveforms depict positive current density measures. (**a**) Source waveforms and localizations for the sensory effects of color (blue tracing) and motion (red tracing). Vertical lines indicate time points when the activity first deviated significantly from baseline, which occurred at 115 ms post-stimulus onset for color ($F_{1,17} = 4.58$, $P = 0.047$) and at 125 ms for motion ($F_{1,17} = 4.55$, $P = 0.047$). (**b**) Averaged source activity waveforms for motion-sensitive sources in the middle occipital gyri (red tracing) and color-sensitive sources in inferior occipital cortex (blue tracing) from experiment 1, in which selection of the surface was based on motion speed. Note that the onset of relevant motion-selective activity occurred at 155 ms post stimulus ($F_{1,17} = 4.68$, $P = 0.045$), whereas the object-based selection of the task-irrelevant color feature began 60 ms later ($F_{1,17} = 4.6$, $P = 0.046$). (**c**) Averaged source activity waveforms for motion-sensitive sources in the middle occipital gyri (red trace) and color-sensitive sources in inferior occipital cortex (blue trace) from experiment 2, where the attentional selection of the surface was based on color. In contrast with experiment 1, the color-selective enhancement occurred first (starting at 160 ms) ($F_{1,11} = 4.86$, $P = 0.049$) and the object-based selection of the irrelevant motion feature occurred 65 ms later at 230 ms ($F_{1,11} = 5.04$, $P = 0.046$).

area. This modulation took the form of an enhanced neural response in the color area when the red (versus gray) surface was attended and in the motion area when the fast-moving (versus the slow moving) surface was attended. Finally, selection of the task-irrelevant feature was indexed after a further delay of 60–65 ms by an additional modulation in the corresponding feature-specific cortical area. This rapid sequential activation of the relevant and irrelevant feature modules reveals a basic mechanism for object-based attention that corresponds closely with the predictions of both Duncan's integrated competition model[7,8,18] and Roelfsema's incremental grouping model[10].

The integrated competition model aims to account for findings that different objects in a visual scene compete for attention[7] and are perceived as perceptual units, even though the features of an attended object may be encoded in anatomically separated brain areas. According to this model, directing attention to one of an object's features produces an enhanced response and competitive advantage for the object in the specialized cortical module that encodes the attended feature, which is then transmitted to the modules that encode the other features of the object. The resulting activation of the entire network of specialized modules then accomplishes the binding of features into a unified perceptual object that is highlighted by attention. The incremental grouping theory of feature binding[10] similarly proposes that neurons in the distributed brain areas encoding the features of an attended object show enhanced activity that spreads across a network of inter-areal connections. In particular, feature binding across visual areas occurs by the enabling of recurrent connections between neural populations that belong to the attended perceptual grouping (in our case, the attended moving surface). The time-consuming spread of facilitation through these recurrent connections leads to the explicit representation of the attended object. This mechanism of distributed response enhancement mediated by enabled connections provides an alternative to the binding-by-synchrony hypothesis[19], which has received mixed support[10,20].

Our results fit with these models in two important ways. First, source analysis of the feature-selective neural activity revealed that the estimated anatomical generators were virtually identical for the initial sensory registration and for both the relevant and irrelevant feature selections. The Talairach coordinates of these sources corresponded to the well-known color area V4/V8 in the ventral-fusiform gyrus[17,21,22] and the motion area MT/V5 in the middle occipital gyrus[23,24], respectively. Second, the delay interval between the activations of the relevant and irrelevant feature modules fits with the proposal that the object first becomes dominant in the relevant feature module and then spreads to the modules encoding the irrelevant features of the object. Thus, these data support the basic tenet of the integrated competition and incremental grouping models, namely that a unitary perceptual object can be constructed through the sequential selection and binding of its relevant and irrelevant attributes in their specialized cortical modules. Moreover, the ERF source waveforms provide specific information about the timing of the inter-areal binding processes, with relevant and irrelevant feature selections becoming separated by 60–65 ms.

Our MEG data are also consistent with neurophysiological studies in non-human primates, which have shown that directing attention to the color of a moving surface produces an enhanced firing of cells in the motion area MT that was selectively responsive to the direction of movement of the attended surface[25,26]. These animal studies are consistent with object-based theories of attention that propose a transfer of attention from relevant to irrelevant features in an attended object. Our results in humans extend these findings by showing that the relevant and irrelevant features were selected sequentially in a time-consuming process (that requires of the order of 60–65 ms). Notably, our data are not compatible with an alternative mechanism that was considered previously[26], whereby color and motion would be grouped pre-attentively into an elementary object representation, and attention would select both the relevant and irrelevant features at the same time.

According to the feature integration theory, an object's features become bound together into a unified percept when spatial attention is directed to the object's location[27]. Further evidence that spatially directed attention contributes to object-based selection comes from both behavioral[28–30] and physiological[31–35] studies showing that attention directed to one location in an object can spread throughout the entire object and facilitate the processing of stimuli in its boundaries. In our experiments, however, it does not seem possible that spatial attention could be directed selectively to one of the two dense, overlapping arrays of moving dots, which could only be distinguished by their motion speed and/or color features. Previous studies

have also demonstrated that attention can be allocated selectively to one of two spatially overlapped stimuli on the basis of their shape[11,36], color[37] or direction of motion[12,14,16,38,39] features. It appears then that both feature-selective and spatially directed attention are important for the selection of perceptual objects, but under different circumstances (for example, when attending to spatially overlapped versus non-overlapped objects). Further work is needed to discover whether there are communalities in the neural mechanisms by which feature and spatial attention enhance object perception.

Our MEG recordings reinforce the view that objects are the basic units of attention and identify a specific neural mechanism by which object-based selection may be achieved. These findings are consistent with the central hypothesis of the integrated competition and incremental grouping models of object-selective attention, namely that selection of an object by attending to one of its features is accomplished by the sequential activation of the relevant and irrelevant feature modules. The results of experiments 1 and 2 indicate that the order of feature selections is highly flexible and dependent on the top-down task instructions. Although questions still remain about the nature of the neural operations that bind the activations of the relevant and irrelevant feature modules into a unified perceptual object[9,11,20], our results provide crucial information on the timing of feature selection and binding processes that must be taken into account by both neural and psychological models of object-selective attention.

METHODS

Methods and any associated references are available in the online version of the paper.

Note: Any Supplementary Information and Source Data files are available in the online version of the paper.

ACKNOWLEDGMENTS

We would like to thank M. Wachter for help with the data collection and N. Nönnig and M. Scholz for technical support. This work was supported by grants Scho1217/1-2 and SFB779 TP A1 from the Deutsche Forschungsgemeinschaft (DFG) and by grants from the US National Science Foundation (BCS-1029084) and the National Institute of Mental Health (1P50MH86385).

AUTHOR CONTRIBUTIONS

M.A.S. designed and performed the experiments, analyzed the data and wrote the paper. J.-M.H. designed the experiments and analyzed the data. C.M. analyzed the data. H.-J.H. supervised the performance of the experiments and data analysis. S.A.H. designed the experiments, supervised the performance of the experiments and data analysis, and wrote the paper.

COMPETING FINANCIAL INTERESTS

The authors declare no competing financial interests.

1. Posner, M.I., Snyder, C.R.R. & Davidson, B.J. Attention and the detection of signals. *J. Exp. Psychol.* **109**, 160–174 (1980).
2. Wolfe, J.M. Guided search 2.0 A revised model of visual search. *Psychon. Bull. Rev.* **1**, 202–238 (1994).
3. Chen, Z. Object-based attention: a tutorial review. *Atten. Percept. Psychophys.* **74**, 784–802 (2012).
4. Scholl, B.J. Objects and attention: the state of the art. *Cognition* **80**, 1–46 (2001).
5. Boehler, C.N., Schoenfeld, M.A., Heinze, H.-J. & Hopf, J.-M. Object-based selection of irrelevant features is not confined to the attended object. *J. Cogn. Neurosci.* **23**, 2231–2239 (2011).
6. Hopf, J.M., Heinze, H.J., Schoenfeld, M.A. & Hillyard, S.A. Spatio-temporal analysis of visual attention. in *The Cognitive Neurosciences IV* (ed. Gazzaniga, M.S.) 235–250 (MIT Press, Cambgridge, Massachusetts, 2009).
7. Desimone, R. & Duncan, J. Neural mechanisms of selective visual attention. *Annu. Rev. Neurosci.* **18**, 193–222 (1995).
8. Duncan, J. Selective attention and the organization of visual information. *J. Exp. Psychol. Gen.* **113**, 501–517 (1984).
9. Duncan, J., Humphreys, G.W. & Ward, R.M. Competitive brain activity in visual attention. *Curr. Opin. Neurobiol.* **7**, 255–261 (1997).
10. Roelfsema, P.R. Cortical algorithms for perceptual grouping. *Annu. Rev. Neurosci.* **29**, 203–227 (2006).
11. O'Craven, K.M., Downing, P.E. & Kanwisher, N. fMRI evidence for objects as the units of attentional selection. *Nature* **401**, 584–587 (1999).
12. Schoenfeld, M.A. *et al.* Dynamics of feature binding during object-selective attention. *Proc. Natl. Acad. Sci. USA* **100**, 11806–11811 (2003).
13. He, Z.J. & Nakayama, K. Visual attention to surfaces in three-dimensional space. *Proc. Natl. Acad. Sci. USA* **92**, 11155–11159 (1995).
14. Valdes-Sosa, M., Cobo, A. & Pinilla, T. Transparent motion and object-based attention. *Cognition* **66**, B13–B23 (1998).
15. Valdes-Sosa, M., Cobo, A. & Pinilla, T. Attention to object files defined by transparent motion. *J. Exp. Psychol. Hum. Percept. Perform.* **26**, 488–505 (2000).
16. Schoenfeld, M.A. *et al.* Spatio-temporal analysis of feature-based attention. *Cereb. Cortex* **17**, 2468–2477 (2007).
17. Rodríguez, V., Valdes-Sosa, M. & Freiwald, W. Dividing attention between form and motion during transparent surface perception. *Brain Res. Cogn. Brain Res.* **13**, 187–193 (2002).
18. Duncan, J. in *Attention and Performance XVI* (ed. McClelland, J.L.) 549–578 (MIT Press, Cambridge, Massachusetts, 1996).
19. Singer, W. Neuronal synchrony: a versatile code for the definition of relations? *Neuron* **24**, 49–65, 111–125 (1999).
20. Palanca, B.J. & DeAngelis, G.C. Does neuronal synchrony underlie visual feature grouping? *Neuron* **46**, 333–346 (2005).
21. Hadjikhani, N., Liu, A.K., Dale, A.M., Cavanagh, P. & Tootell, R.B. Retinotopy and color sensitivity in human visual cortical area V8. *Nat. Neurosci.* **1**, 235–241 (1998).
22. Zeki, S., McKeefry, D.J., Bartels, A. & Frackowiak, R.S. Has a new color area been discovered? *Nat. Neurosci.* **1**, 335–336 (1998).
23. Seymour, K., Clifford, C.W., Logothetis, N.K. & Bartels, A. The coding of color, motion and their conjunction in the human visual cortex. *Curr. Biol.* **19**, 177–183 (2009).
24. Stoppel, C.M. *et al.* Feature-based attention modulates direction-selective hemodynamic activity within human MT. *Hum. Brain Mapp.* **32**, 2183–2192 (2011).
25. Katzner, S., Busse, L. & Treue, S. Attention to the color of a moving stimulus modulates motion-signal processing in macaque area MT: evidence for a unified attentional system. *Front. Syst. Neurosci.* **3**, 12 (2009).
26. Wannig, A., Rodriguez, V. & Freiwald, W.A. Attention to surfaces modulates motion processing in extrastriate area MT. *Neuron* **54**, 639–651 (2007).
27. Treisman, A. Feature binding, attention and object perception. *Phil. Trans. R. Soc. Lond. B* **353**, 1295–1306 (1998).
28. Egly, R., Driver, J. & Rafal, R.D. Shifting visual attention between objects and locations: evidence from normal and parietal lesion subjects. *J. Exp. Psychol. Gen.* **123**, 161–177 (1994).
29. Goldsmith, M. & Yeari, M. Central-cue discriminability modulates object-based attention by influencing spatial attention. *Exp. Psychol.* **59**, 132–137 (2012).
30. Law, M.B. & Abrams, R.A. Object-based selection within and beyond the focus of spatial attention. *Percept. Psychophys.* **64**, 1017–1027 (2002).
31. He, X., Fan, S., Zhou, K. & Chen, L. Cue validity and object-based attention. *J. Cogn. Neurosci.* **16**, 1085–1097 (2004).
32. Kasai, T. Attention-spreading based on hierarchical spatial representations for connected objects. *J. Cogn. Neurosci.* **22**, 12–22 (2010).
33. Martínez, A., Teder-Salejarvi, W. & Hillyard, S.A. Spatial attention facilitates selection of illusory objects: evidence from event-related brain potentials. *Brain Res.* **1139**, 143–152 (2007).
34. Martínez, A. *et al.* Objects are highlighted by spatial attention. *J. Cogn. Neurosci.* **18**, 298–310 (2006).
35. Muller, N.G. & Kleinschmidt, A. Dynamic interaction of object- and space-based attention in retinotopic visual areas. *J. Neurosci.* **23**, 9812–9816 (2003).
36. Zinni, M.M.A. & Hillyard, S.A. The neural basis of color binding to an attended object. in *Electrophysiology of Attention: Signals of the Mind* (ed. Mangun, G.R.) (Elsevier, New York, 2013).
37. Sohn, W., Papathomas, T.V., Blaser, E. & Vidnyanszky, Z. Object-based cross-feature attentional modulation from color to motion. *Vision Res.* **44**, 1437–1443 (2004).
38. Khoe, W., Mitchell, J.F., Reynolds, J.H. & Hillyard, S.A. Exogenous attentional selection of transparent superimposed surfaces modulates early event-related potentials. *Vision Res.* **45**, 3004–3014 (2005).
39. Reynolds, J.H., Alborzian, S. & Stoner, G.R. Exogenously cued attention triggers competitive selection of surfaces. *Vision Res.* **43**, 59–66 (2003).

ONLINE METHODS

Subjects. 18 healthy subjects (8 male, ages 22–32 years) with normal color vision and normal or corrected-to-normal acuity participated as paid volunteers in experiment 1; 12 additional subjects (6 male, ages 19–29) participated in experiment 2. All gave informed consent, and the study was approved by the ethics committee of the medical faculty of the Otto-von-Guericke University, Magdeburg, Germany. The minimum sample size of $N = 10$ was calculated on the basis of the modulation of the ERF effects in one of our previous studies[12] in which we investigated the effects of object-based attention on the processing of a task irrelevant object feature (color).

Stimuli. In both experiments, moving dot stimuli were presented via a projector/mirror system at a fixed distance of 120 cm in front of the subject. Stimuli were presented against a dark background (0.22 cd m^{-2}) in a square aperture (4° × 4°) that was centered on the vertical meridian and situated 3° above a central fixation cross (to the lower edge of the square). 100 stationary gray dots (220 cd m^{-2}) were continuously present in this aperture during the inter-trial intervals. At the start of each trial, half of the dots moved coherently downwards with a speed of 4° s^{-1} for 300 ms while the other half moved simultaneously in the same direction with a speed of 7° s^{-1}. Each dot population was uniformly colored and perceived as a moving transparent surface. In experiment 1, the color of one transparent surface was maintained as gray (the same as in the inter-trial interval), whereas the other surface was either maintained as gray or changed to an isoluminant red at the onset of the 300-ms period of movement and then changed back to gray after the movement ceased (**Fig. 6a**,**b**). In experiment 2, the color of one of the surfaces changed to red during the movement interval, whereas the other surface was maintained as gray (**Fig. 6c**,**d**). Red/gray isoluminance was established through heterochromatic flicker photometry. In a separate experimental session, each subject was presented with two 2 × 2° squares adjacent to the vertical meridian and 2° above a fixation cross that was located in the center of the display. One square was gray (the same gray as the dots that didn't change color), whereas the other square was red, and their presentation was alternated at 12 Hz. Subjects pressed a button to change stepwise the intensity of the red square until the perceived flickering was minimal.

In experiment 1, the task of the subjects was to attend either to the fast- or slow-moving surface. The color of the slow (4° s^{-1}) or fast (7° s^{-1}) moving dots could be either red or white on an unpredictable, pseudo-random basis, leading to three basic stimulus combinations (**Fig. 1a**): red-slow/gray-fast, gray-slow/red-fast and gray-slow/gray-fast. Also on a pseudo-random basis (30% of the trials), either the slow or the fast moving dots were subject to a small horizontal translation that served as a target. The inter-trial interval varied randomly between 1.2–2.0 s, after which the 100 stationary dots were randomly re-assigned to either the slow or fast moving surfaces. In the inter-trial interval, the color of all the dots was gray.

In experiment 2, subjects were cued to attend to either the red or the gray surface regardless of their speeds. As in experiment 1, the task was to press a button after detecting a horizontal displacement of the attended surface. In experiment 2, however, the number of stimulus combinations was reduced to either red-slow/gray-fast or gray-slow/red-fast, and attention was directed to one or the other surface solely on the basis of its color (gray or red). All other stimulus properties were the same as in experiment 1.

Procedure. Prior to each block of 18 trials in experiment 1, a symbolic cue (single or double arrow pointing downwards) replaced the fixation cross for 2 s indicating to the subjects which movement speed (that is, either the fast- or slow-moving surface) was to be attended on that block. During each block a target stimulus (small horizontal translation in the attended surface) could occur on 1–3 trials at random. Horizontal translations could also occur 1–3 times per block in the unattended surface, but these were not targets and were to be ignored. Subjects were instructed to press a button as quickly as possible after detecting a target. In experiment 1, the colors of the dots were irrelevant to the assigned task, and the cue indicated which transparent surface had to be attended on the basis of the speed of the surface.

In experiment 2, the dots of one of the transparent surfaces were always colored red and those of the other surface always gray. Here, the cue indicated which surface had to be attended on the basis of its color (gray or red arrow pointing downwards). After 18 trials, a new cue appeared, which was followed by the next block of trials. Each experimental run consisted of ten blocks and had a duration of 6–7 min.

Prior to the experimental sessions, the subjects were trained to maintain fixation and were familiarized with the task for about 45 min. Fixation was verified with vertical and horizontal electrooculogram recordings that have a resolution of about 1°. The importance of maintaining fixation was emphasized, and the subjects broke fixation during the recordings on less than 1% of the trials.

ERF recordings. ERFs were recorded using a BTI Magnes 2500 WH (4D Neuroimaging) whole-head system with 148 magnetometer channels. Recording bandpass was DC-50 Hz with a sampling rate of 254 Hz. Artifact rejection was performed off-line by removing trials with peak-to-peak amplitudes exceeding a threshold of 3.0×10^{-12} T (about 2% of the trials), as well as non-target trials where button presses erroneously occurred (<1% of the trials). This procedure eliminated all trials with eye movements. Individual head shapes were co-registered with the sensor coordinate system by digitizing (Polhemus 3-Space Fastrak) skull landmarks (nasion, left and right preauricular points) and determining their locations relative to sensor and electrode positions using signals from five distributed head coils. These landmarks enabled co-registration of ERP/ERF activity with individual anatomical MR scans. Fixation was verified with vertical and horizontal electrooculogram recordings.

ERF waveforms time-locked to motion onset were averaged separately for each of the trial types. In experiment 1, there were three stimulus conditions × two attention conditions (**Fig. 1a**). In experiment 2, there were two stimulus conditions × two attention conditions (**Fig. 1b**). Only ERFs elicited by the more frequent non-target stimuli (without horizontal translation) were analyzed here.

In experiment 1, the sensory effect of the presence of color was revealed in difference waves formed by subtracting the ERF waveforms elicited by the no color-change (gray-slow*/gray-fast) trials from those elicited by the unattended color change (gray-slow*/red-fast) trials. The sensory effect of motion was taken as the first deflection in the ERF elicited by gray-slow*/gray-fast trials. The sequential selections of the relevant motion feature (fast versus slow) and of the irrelevant color feature (red versus gray) were revealed in two additional ERF difference wave comparisons: (1) the ERF on gray-slow*/red-fast trials was subtracted from the ERF on gray-slow/red-fast* trials, and (2) the ERF on gray-fast/red-slow* trials was subtracted from the ERF on gray-fast*/red-slow trials. In both of these difference wave comparisons, the ERF indexing the initial selection on the basis of the relevant motion-speed feature (attend-fast minus attend-slow) and the subsequent ERF indexing selection of the irrelevant color feature could be visualized.

In experiment 2, where the surfaces were selected on the basis of color (red versus gray) the critical difference wave comparisons were as follows: (1) the ERF on red-fast/gray-slow* trials was subtracted from the ERF on red-fast*/gray-slow trials, and (2) the ERF on red-slow/gray-fast* trials was subtracted from the ERF on red-slow*/gray-fast trials. Both of these difference wave comparisons revealed the ERF indexing the initial selection on the basis of the relevant color feature (attend-red minus attend-gray), followed by the ERF indexing selection of the irrelevant motion feature.

As the data was normally distributed (with similar variances between the conditions), the statistical analyses of the above mentioned effects indexing the selection of the relevant and irrelevant features were performed using repeated-measures ANOVAs on the amplitudes of the ERF raw waveforms. These were quantified as mean amplitude measures over specified latency intervals (with respect to a 200-ms pre-stimulus baseline) at the sensor sites (averages of three neighboring sensors) showing the largest amplitude modulations as a function of attention and tested with repeated-measures analysis of variance. Two-tailed tests were used throughout. Multiple comparisons were not performed. The locations of the sensor groups are indicated by the black circles on the topographical distribution maps of the magnetic fields in **Figures 2**–**5**. To determine the time of onset of the sensory and attention effects, amplitude measures were taken over windows of 10 ms that were slid sequentially in time in 3.9-ms steps and tested for deviation from baseline with a criterion of $P < 0.05$ (ref. 40). The earliest significant interval followed by five (or more) successive significant intervals was taken as the onset latency[9,14,15,17].

Source analysis was carried out using multi-modal neuroimaging software (Curry 6.0, Neuroscan) on the difference waveforms shown in **Figures 4** and **5**. Source modeling was performed using minimum norm estimates constrained to the cortical surface in a realistic boundary element model (BEM) of each subject's head derived from magnetic resonance imaging. For the grand averaged data,

the BEM was derived from the MNI brain. In the source analyses all sensory and attention-related ERF modulations for color were localized to a ventral-occipital region (inferior occipital cortex), whereas all sensory and attention effects for motion were localized to a lateral occipital region (middle occipital gyri), in accordance with previous reports[17].

Source time courses (see **Fig. 6**) were extracted from the data using an algorithm in which a region of interest (sphere with a radius of 0.5 cm) was placed on the maximum focus of activity of each of the four estimated sources (that is, in the above-mentioned ventral and lateral occipital areas of the left and right hemispheres). For each of these sources, the time course of activity within the region of interest was individually extracted over the time range −50–440 ms after motion onset. Given that minimum norm estimates are based on current density measures constrained to the cortical surface, the obtained values are always positive. In experiment 1, the time course calculations for motion selection followed by color selection were based on the source analyses performed on two difference waveforms: (1) ERF on gray-slow*/red-fast trials subtracted from ERFs on gray-slow/red-fast* trials, and (2) ERFs on gray-fast/red-slow* trials subtracted from ERFs on gray-fast*/red-slow trials). The source activity time courses for these two difference waves were averaged together for each of the four regions. After determining the maximal amplitudes and the onset latencies using the sliding window method (see above), the data from homologous left and right hemisphere sources were submitted to separate repeated-measures ANOVAs with the factor hemisphere. No significant hemispheric differences were found, either for the onset latency ($F_{1,35} = 0.82$, $P = 0.37$ for the ventral occipital; $F_{1,35} = 0.46$, $P = 0.5$ for the lateral occipital sources) or for the amplitude ($F_{1,35} = 0.68$,$P = 0.42$ for the ventral occipital; $F_{1,35} = 0.34$, $P = 0.56$ for the lateral occipital sources). Consequently, the source activity time courses for the homologous bilateral regions were averaged across hemispheres, thereby resulting in one time course for the ventral occipital and a second one for the lateral occipital region. The time course of source activity of the sensory motion effect was based on the source analysis performed on the first deflection in the ERF elicited by gray-slow*/gray-fast trials, while for the sensory color effect the source time course was established from the analysis performed on the difference between gray-slow*/red-fast minus gray-slow*/gray-fast trials.

For experiment 2, the calculation of the time courses for color selection followed by motion selection was also based on the source analyses performed on two difference waveforms: (1) the ERF on red-fast/gray-slow* trials subtracted from the ERF on red-fast*/gray-slow trials, and (2) the ERF on red-slow/gray-fast* trials subtracted from the ERF on red-slow*/gray-fast trials. As for the first experiment these two source activity time courses were first averaged together separately for each region (ventral and lateral occipital). Again, no significant differences were found between homologous left and right hemispheric sources, either for the latencies, or for the amplitudes (onset latency: $F_{1,23} = 0.68$, $P = 0.42$ for the lateral occipital; $F_{1,23} = 1.54$, $P = 0.23$ for the ventral occipital sources); amplitude: ($F_{1,23} = 2.14$, $P = 0.16$ for the lateral occipital; $F_{1,23} = 2.84$, $P = 0.11$ for the ventral occipital sources). Consequently, the time courses for the ventral and the lateral occipital regions were averaged individually and then across hemispheres. To determine the onsets of the source activity, mean amplitudes of the source waveforms were again calculated over successive 10-ms intervals and tested for deviation from baseline ($P < 0.05$ criterion). The first of five or more consecutive intervals meeting this criterion was considered the onset time. These criteria were also used to test the differences in latency between the relevant and irrelevant source waveform modulations in experiments 1 and 2 (see **Fig. 6**).

40. Guthrie, D. & Buchwald, J.S. Significance testing of difference potentials. *Psychophysiology* **28**, 240–244 (1991).

doi:10.1038/nn.3656